A MAGNETICALLY ENHANCED 3-ELECTRODE WIRELESS MICRO-GEIGER COUNTER

Christine K. Eun[1], Tze-Ching Fung, Bhaskar Mitra, and Yogesh B. Gianchandani
Center for Wireless Integrated Microsystems (WIMS)
Department of Electrical Engineering and Computer Science, University of Michigan
[1]1301 Beal Avenue, Ann Arbor, Michigan, USA, e-mail: eunc@umich.edu

ABSTRACT

This paper explores a 3-electrode micromachined Geiger counter utilizing a high impedance (floating) electrode to control discharge energy, and its impact on sensitivity and response time. Permanent magnets in a sandwich configuration are used to enhance RF transmission from micro-discharges. Initially, weak (field-emission) leakage current charges the floating electrode capacitor ($C_P \approx 1.1$ pF) to a high voltage through the *charging gap* (between floating electrode and anode). When beta radiation initiates a micro-discharge in the *sensing gap* (between floating electrode and cathode), C_P dissipates through the low impedance path, lowering the voltage and quickly quenching the discharge. Permanent magnets, positioned perpendicular to the discharge path, increase the efficiency of electron-ion collisions and enhance the consequent RF transmission. Experiments conducted in a neon/air ambient with ^{90}Sr (0.1 μCi) showed a 10X-100X SNR improvement for the 3-electrode design over a similar 2-electrode design that does not utilize the floating electrode. Results also showed a significant increase in high frequency components in the presence of a magnetic field.

I. INTRODUCTION

Previous efforts on lithographically microfabricated radiation detectors have included solid-state, scintillator-based, and gas-based devices [1-8]. Gas-based detectors, such as the Geiger counter, are the preferred sensors for detecting beta radiation, because they are reliable, temperature insensitive, require only simple circuitry, and measure over a much wider range of radiation species and energies. Recent work has reported micromachined Geiger counters fabricated from a glass-Si-glass stack [9].

Wireless communication using gas-based discharges were employed in the mid-1890's with Guglielmo Marconi's spark gap transmitters [10]. The discharge gaps were relatively large (on the order of cm), achieving transmission distances on the order of kilometers. In 1901, Bose utilized these discharges within waveguides in order to generate microwaves, and more recent activity has also been reported [11]. Beta particle-initiated micro-discharges from a gas-based micromachined Geiger counter have been shown to emit radio-frequency signals in the ultra wideband (UWB) frequency range [12]. This inherent wireless signal was found to span more than 3 GHz without the need for additional electronics [13]. This is potentially advantageous from the viewpoint of wireless sensor networking. Studies with the MicroGeiger investigating the influence of the bias circuitry have demonstrated that by varying certain passive components, the resulting RF spectra can be shaped and tailored, extending the technology to the application of sensor networks [14]. Networked radiation sensors are envisioned for monitoring public buildings with high pedestrian traffic such as train stations, environmental hazards, and inaccessible terrains.

Large permanent magnets in plasma magnetron systems for micromachining have been widely employed in sputtering deposition systems. Traditionally, plasma magnetrons made use of powerful magnets to increase plasma density and consequently increase sputtering efficiency. The mean free path is relatively large (on the order of a few cm) due to operation at lower pressures (on the order of 5-10 mTorr of pressure) [15]. Miniaturized permanent magnets have been utilized in the past to enhance and confine dc microplasmas to enable localized, maskless etching of silicon with SF_6 gas [16]. More recently, studies integrating small rare earth magnets with Si/glass micromachined radiation sensors have shown an enhancement in the received wireless signal [17].

Multi-electrode geometries for chemical detection of vapors at atmospheric pressure have been explored [18]. Utilizing a high-impedance middle electrode, the three-terminal FlashFET was able to achieve lower power discharges (22.5 μJ/pulse) at high speeds and without loss in spectral resolution. The device comprised three planar Cu electrodes with an active area of 1 mm^2. Copper electrodes tend to outperform doped silicon electrodes for discharge applications by having lower sheet resistance and higher durability and lifetime. One problematic aspect of micro-electrodes is the tendency to wear, which results from sputtering. This limits device lifetime and can lead to inconsistent device operation.

This paper presents a magnetically enhanced, 3-electrode wireless micromachined Geiger counter. The device uses miniature rare earth magnets (NdFeB) integrated with planar Cu electrode geometries to produce wireless transmissions in the UWB window. Section II describes the concepts realized in the 2- and 3-electrode micro-Geiger counter device, the employment of permanent magnets to enhance RF transmission, and finally the FEA of the electric field profile during device operation. Section III presents the recent experimental results comparing pulse height spectra obtained from the 2- and 3-electrode device operation, and the magnetic enhancement of the wireless signal with the 3-electrode device. Section IV concludes with a discussion of possible applications.

II. DEVICE CONCEPTS

This section first describes the power saving operation with the 3-electrode configuration, and then presents a

theory of how signal enhancement is achieved with the magnetic configuration.

Device Configuration

There are two electrode configurations of interest: 2- and 3-electrode geometries that use closely spaced Cu electrodes electroplated on an insulating glass substrate. The main interest involves the 3-electrode device that uses a high impedance (floating) electrode that remains unwired. The *sensing gap* (Fig. 1) located between the cathode and floating electrode has a relatively large interaction area (200X500 μm^2) and a high electric field (1-2 MV/m). Initially, weak (field-emission) leakage current charges the capacitor (C_P) to a high voltage through the *charging gap,* located between the floating electrode and anode. When beta radiation initiates a micro-discharge within the *sensing gap*, the charge on C_P (≈1.1 pF) is dumped through the low impedance path, lowering the applied voltage and quickly quenching the discharge. Consequently, it results in rapid current switching, which is favorable for RF generation, because it increases the time derivative of current pulses. Also, the resulting current pulses are smaller, decreasing the operating energy and temperature of the electrodes, reducing the sputtering effect noted previously. This decreases electrode wear and extends the lifetime compared to the 2-electrode configuration.

The 2-electrode device involves the *sensing gap* alone. The floating electrode is hardwired to serve as the anode connection, while the cathode is still grounded. The 2-electrode geometry is used as a control to compare performance with the 3-electrode device under similar experimental conditions.

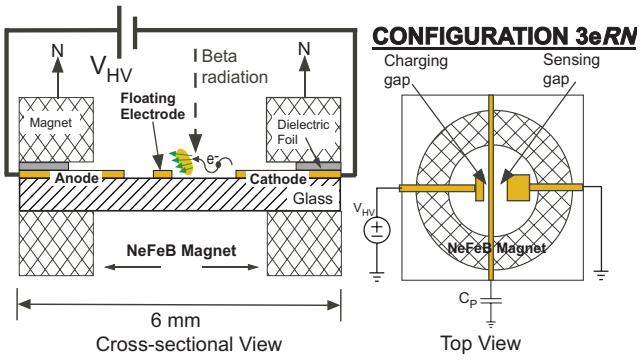

Fig. 1: Cross-section of device in Configuration 3e*RN*. Each ring magnet measured 6 mm outer diameter and 3 mm inner diameter. The 3-electrode micro-Geiger counter is fabricated on Pyrex #7740 substrate with 25 μm thick electroplated Cu electrodes. The *charging gap* and *sensing gap* are shown on the right.

There are a number of compromises related to the size of C_P (e.g. dynamic range versus recovery time). While C_P is discharging, the device is essentially unable to detect more incoming particles, this is known as "dead time." Consequently, with a large C_P, the device is able to detect a large influx of beta particles without lowering the operating voltage. However, past studies have shown that a smaller C_P results in a larger RF transmission, due to the faster current switching profile.

Magnetic Enhancement Configuration

The device also involves an arrangement of permanent magnets (NdFeB) that significantly enhances the RF generation. The idea is similar to a magnetron, where magnets suppress wall collisions and increase the efficiency of the electro-discharges. The ring-shaped magnets sandwich the 3-electrode device. The top magnet is electrically isolated from the Cu electrodes by an insulating spacer. The second magnet located below the glass substrate is used to stabilize the arrangement. The magnetic field lines are positioned perpendicular to the discharge path. A particle that is moving in the presence of both an electric field and an orthogonal magnetic field, B_0, which is also consequently perpendicular to the discharge path, will give rise to a drift velocity, v_F, perpendicular to both fields:

$$v_F = \frac{(\mathbf{F}_\perp / q) \times \mathbf{B}}{B_0^2} \qquad (1)$$

$F_\perp$ represents the transverse force due to the electric field acting on the particle. **B** is the component of the magnetic field that is orthogonal to the electric field and q represents the charge. The particle velocity is directly proportional to the applied magnetic field. The particle will experience a gyrating motion, much like a spiral coil course, around this new, elongated discharge path [19]. Since each accelerating particle emits electromagnetic radiation, increasing the number of excited atoms can generate a stronger overall signal. In essence, this new discharge path provides an opportunity for more ion-to-neutral gas atom collisions, and thereby creates more ionized particles that can participate in the wireless transmission. Photographs of the 3-electrode micro-Geiger counter incorporating permanent magnets (Configuration 3e*RN*) are shown in Fig. 2.

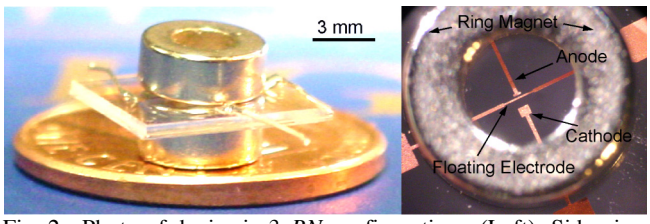

Fig. 2: Photo of device in 3e*RN* configuration. (Left) Side view of 3-electrode radiation sensor in magnetic sandwich against a U.S. penny. (Right) Top view of the 3-electrode device shown through magnet opening.

Finite Element Analysis (FEA)

FEA of the electric field profile is performed on the 3-electrode arrangement (Fig. 3). The anode potential was set to 550 V, while the cathode was tied to ground. The average field in the *sensing gap* for the 3-electrode configuration is greater than 1.2 MV/m, which is sufficient for beta particle detection. In typical gases at atmospheric pressure, the threshold field required for operation is on the order of 10^6 V/m [20]. Generally, Geiger counters operate with electric fields (near the high field anode wire) of around a few MV/m.

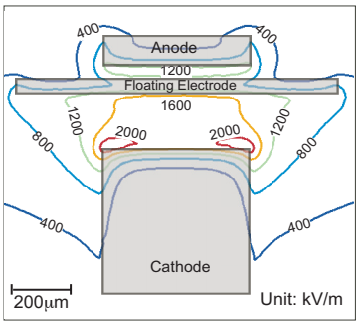

Fig. 3: FEM simulation of the electric field profile for the 3-electrode device. The data was extracted from a plane that is 50 μm above the substrate surface. The anode potential was set to 550 V, while the cathode was tied to ground.

III. EXPERIMENTAL RESULTS

Tests were conducted in a neon-filled environment while sensing a 0.1 μCi ^{90}Sr sample (Fig. 4). The dimensions for the sensing and charging gaps were 200 μm and 50 μm, respectively. For wireless measurements, an 800 MHz whip antenna was attached to the spectrum analyzer. Figure 5 shows the antenna gain factor supplied by the manufacturer (Protek, Inc.) from 100 MHz to 2 GHz. This characterization covers a significant portion of the frequency bandwidth of interest (200 MHz to 2.9 GHz). However, the antenna gain factor was not taken into account in wireless data provided here.

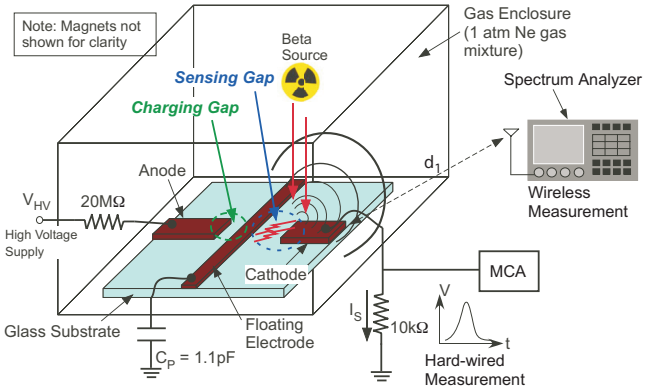

Fig. 4: Test setup showing the spectrum analyzer (HP8592L) with device bias circuitry. Source-to-detector distance was fixed at 8 mm while detector-to-antenna distance, d_1, was varied from 5 to 80 cm. All tests are operated in a neon/air gas environment at 1 atm. Applied voltage (V_{HV}) was between 400 - 800 V.

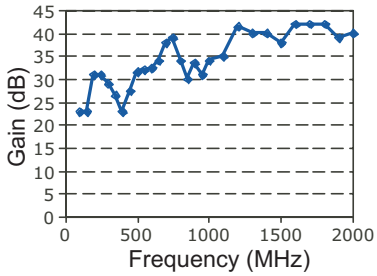

Fig. 5: Antenna gain factor for the 800 MHz whip antenna used for the wireless measurement setup. Data was provided by the manufacturer (Protek, Inc.) for the frequencies spanning 100 MHz to 2 GHz.

3-Electrode Configuration

For hard-wired measurements, avalanche current pulses (I_S) were measured by a high-speed pico-ammeter for over 100 s during device operation (Fig. 6). The 3-electrode arrangement clearly shows a 10X reduction in pulse amplitudes as well as a faster response compared to the corresponding 2-electrode device. The pulse reduction permits lower operating power and longer lifetime for the 3-electrode device. Figure 7 shows signal-to-noise ratios (SNR) of devices with 2- and 3-electrode arrangements from pulse height spectra measured using a multi-channel analyzer (MCA). SNR is defined as the ratio of count rates with and without a radiation source present. Count rates without a source present involve spontaneous electrostatic discharges (ESD) and background radiation. ESDs tend to occur more frequently when the applied voltage exceeds or nears the gas breakdown voltage. The 3-electrode device produced a higher SNR compared to that of the 2-electrode device over the measured range of anode bias (400-525 V). A higher SNR for the 3-electrode device allows more reliable operation at a wider range of bias voltages.

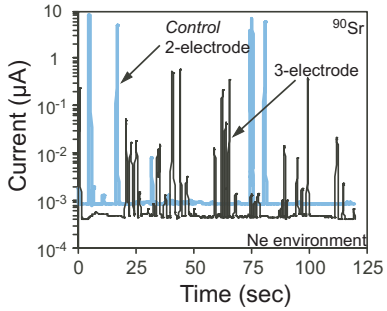

Fig. 6: Hard-wired measurement. Current pulses were measured by a fast pico-ammeter (Keithley 486). The 3-electrode arrangement shows more than a 10X reduction of the current pulse amplitudes as well as an increase in device response and recovery time. The control involved the 2-electrode configuration.

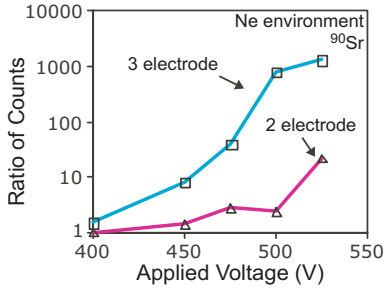

Fig. 7: Hard-wired measurement. Measured signal to background noise ratio (SNR) of different electrode arrangements for applied voltage range: 400-525 V. The 3-electrode device shows 10X-100X order of SNR improvement over the 2-electrode design.

Magnetic Enhancement Configuration

Figure 8 shows the magnetically enhanced RF spectra produced while detecting ^{90}Sr in configuration 3e*RN* compared to spectra produced in the absence of magnets (Control). A significant increase in high frequency spectral strength and bandwidth were achieved in the presence of the magnetic field. The total radiated power decays exponentially (Fig. 9) with increasing detector-to-antenna distance, d_1.

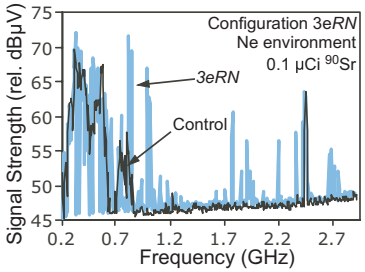

Fig. 8: Wireless measurement. Discharge spectra of beta-initiated breakdown using ^{90}Sr (0.1 μCi). Significant increase in high frequency spectral strength was achieved with the magnetic field present. The frequency sweep spanned from 200 MHz-2.9 GHz.

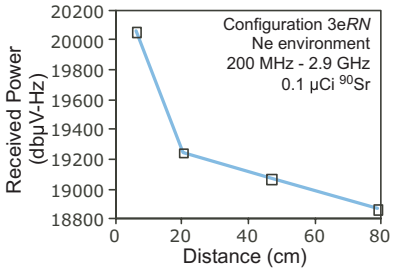

Fig. 9: Wireless measurement. Measured signal attenuation of total received signal power spanning from 200 MHz to 2.9 GHz as a function of detector-to-antenna distance, d_1. An extremely weak source of ^{90}Sr (0.1 μCi) was used.

IV. CONCLUSIONS

In this effort, we have described a planar, 3-electrode copper device with a 250X500 μm^2 active footprint electroplated onto a glass substrate between two miniaturized NdFeB ring magnets. The presence of a third, "floating" electrode, improved detector performance by decreasing the resulting current pulses and increasing the switching or recovery speed. Smaller current pulses resulted in less sputtering of the micro-electrodes, which increased device performance and reliability. The faster switching time increased the spectral strength of the consequent RF transmission since it is directly related to the derivative of the current pulse.

Utilizing miniaturized magnets to considerably increase the inherent emission characteristics of discharge-based transducers would be a significant step in wireless sensor networking. The presence of the magnetic field induces a drift velocity of the electrons and ions that is perpendicular to the discharge path. This additional velocity force results in a change in the current discharge behavior that is realized during device operation.

Preliminary results detecting ^{90}Sr (0.1 μCi) with the 3-electrode device showed a 10X reduction in the current pulse amplitudes, as well as an increase in device response and recovery time as compared to the 2-electrode device. Also, the 3-electrode device shows a 10X-100X SNR improvement over the 2-electrode design. Other multi-electrode configurations can be envisioned to further improve device performance and lifetime. In the presence of miniaturized magnets, the RF spectra emitted by the gas discharges spanned a frequency bandwidth of 200 MHz to 2.9 GHz as well as showing a significant increase in high frequency spectral strength. Even though the effect of a magnetic field is weak while operating at atmospheric pressure, the significant difference in the received RF signal in the presence of magnets suggest there is sufficient field interaction, causing signal enhancement. Increasing field strength can offer larger transmission distances and potentially a wider sensing area.

ACKNOWLEDGEMENTS

This work was supported primarily by the Engineering Research Centers Program of the National Science Foundation under Award Number EEC-9986866. The facilities used for this research include the Michigan Nanofabrication Facility (MNF) at the University of Michigan. The authors would like to thank the University of Michigan Rackham Graduate School for travel support funding.

REFERENCES

[1] S.A. Audet, E.M. Schooneveld, S.E. Wouters, M.H. Kim, "High-purity silicon soft x-ray imaging sensor," *Sensors and Actuators*, A22(1-3), pp. 482-486, Mar. 1990

[2] G. Charpak, J. Derre, Y. Giomataris, P. Rebourgeard, "Micromegas, a multipurpose gaseous detector," *Nuclear Instruments & Methods in Physics Research,* A478(1-2), pp 26-36, Feb. 2002

[3] J.A. Kemmer, "Silicon detectors for nuclear radiation," *IEEE Transducers,* A478, pp. 252-257, 1987

[4] M. Wada, J. Suzuki, Y. Ozaki, "Cadmium telluride ß-ray detector," *IEEE Transducers*, 478, pp. 258-261, 1987

[5] R. Wunstorf, "Radiation hardness of silicon detectors: current status," *IEEE Transactions on Nuclear Science,* 44(3), pp. 806-14, June 1997

[6] B.W. Sturm, Z. He, T.H. Zurbuchen, P.L. Koehn, "Investigation of the asymmetric characteristics and temperature effects of CdZnTe detectors," *IEEE Transactions on Nuclear Science*, 52(5), pp. 2068- 2075, Oct. 2005

[7] R. Gonzalez, J.M. Perez, O. Vela, E. De Burgos, "Performance comparison of a large volume CZT semiconductor detector and a $LaBr_3$(Ce) scintillator detector," *Nuclear Science, IEEE Transactions on Nuclear Science*, 53(4), pp. 2409-2415, Aug. 2006

[8] S. Pellegrin, C. Whitney, C.G. Wilson, "A multichannel nanoparticle scintillation microdevice with integrated waveguides for alpha, beta, gamma, x-ray, and neutron detection," in *IEEE Intl. Conference on MEMS, Istanbul*, pp. 682- 685, Jan. 2006

[9] C.G. Wilson, C.K. Eun, Y.B. Gianchandani, "A microfabricated beta-particle detector with dual cavities for energy spectroscopy," in IEEE Intl. Conf. on MEMS, Miami, Jan. 2005

[10] J.E. Brittain, "Electrical engineering Hall of Fame: Guglielmo Marconi," *Proceedings of the IEEE*, 92(9), pp 1501-4, Aug 2004

[11] A.G. Heaton and J.H. Reeves, "Microwave radiation from discharges," *Intl. Conf. on Gas Discharges*, pp 73-77, Sept. 1974

[12] FCC 02-48, First Report and Order, "Revision of Part 15 of the Commission's Rules Regarding Ultra-Wideband Transmission Systems," Feb 14, 2002: http://hraunfoss.fcc.gov/edocs_public/attachmatch/FCC-02-48A1.pdf

[13] C.K. Eun, R. Gharpurey, Y.B. Gianchandani, "Broadband wireless sensing of radioactive chemicals utilizing inherent RF transmissions from pulse discharges," *IEEE Intl. Conf. on Sensors, Irvine*, Nov. 2005

[14] C.K. Eun, R. Gharpurey,Y.B. Gianchandani, "Controlling ultra wideband transmissions from a wireless micromachined Geiger counter," *IEEE Intl. Conf. on MEMS*,pp.570-573, Jan. 2006

[15] C.H. Shon, J.K. Lee, H.J. Lee, Y. Yang, T.H. Chung, "Velocity distributions in magnetron sputter," *IEEE Transactions on Plasma Science*, 26(26), pp 1635-1644, Dec. 1998

[16] C.G. Wilson, Y.B. Gianchandani, "Miniaturized magnetic nitrogen DC microplasmas," *IEEE Transactions on Plasma Science*, 32(1), pp. 282-287, Feb. 2004

[17] C.K. Eun, R. Gharpurey,Y.B. Gianchandani, "A magnetically enhanced wireless micro-Geiger counter," *A Solid-State Sensors, Actuators and Microsystems Workshop*, Hilton Head, Jun. 2006

[18] B. Mitra, Y.B. Gianchandani, "The micromachined flashFET: a low-power, three-terminal device for high speed detection of vapors at atmospheric pressure," *IEEE Intl. Conf. on MEMS*, pp 794-7, Jan. 2005

[19] M.A. Lieberman, A.J. Lichtenberg, *Principles of Plasma Discharges and Materials Processing*, Wiley, 2nd Edition, 2005

[20] G.F. Knoll, *Radiation Detection & Measurement*, Wiley, 2000